Sofosbuvir and its tri-phosphate metabolite inhibit the RNA-dependent RNA polymerase activity of non-Structural protein 5 from the Kyasanur forest disease virus

Mansi Malik, Parvathy Vijayan, Deepak K Jagannath, Rakesh K Mishra, Anirudha Lakshminarasimhan*

Correspondence

Tata Institute for Genetics and Society, NCBS campus, GKVK, Bellary Road, Bengaluru - 560065, KA, India

*Email: anirudha.lakshminarasimhan@gmail.com

Abstract

Kyasanur forest disease is a neglected zoonotic disease caused by a single-stranded RNA-based flavivirus, the incidence of which was first recorded in 1957 in the Southern part of India. Kyasanur forest disease virus is transmitted to monkeys and humans through the infected tick bite of *Haemophysalis spinigera*. Kyasanur forest disease is a febrile illness, which in severe cases, results in neurological complications leading to mortality. The current treatment regimens are symptomatic and supportive, and no targeted therapies are available for this disease. In this study, we evaluated the ability of FDA-approved drugs sofosbuvir (and its active metabolite) and Dasabuvir to inhibit the RNA-dependent RNA polymerase activity of NS5 protein from the Kyasanur forest disease virus. NS5 protein containing the N-terminal methyl transferase domain and C-terminal RNA-dependent RNA polymerase domain was expressed in *Escherichia coli*, and RNA-dependent RNA polymerase activity was demonstrated with the purified protein. The RNA-dependent RNA polymerase assay conditions were optimized, followed by the determination of apparent $K_{m,ATP}$ to validate the enzyme preparation. Half maximal-inhibitory concentrations against RNA-dependent RNA polymerase activity were determined for Sofosbuvir and its active metabolite. Dasabuvir did not show detectable inhibition with the tested conditions. This is the first demonstration of the inhibition of RNA-dependent RNA polymerase activity of NS5 protein from the Kyasanur forest disease virus with small molecule inhibitors. These initial findings can potentially facilitate the discovery and development of targeted therapies for treating Kyasanur forest disease.

Keywords

Kyasanur forest disease, Kyasanur forest disease virus, Non-structural protein 5, RNA-dependent RNA polymerase, Sofosbuvir, Flavivirus

Abbreviations

KFD – Kyasanur forest disease

KFDV – Kyasanur forest disease virus

NS5 – Non-structural protein 5

RdRp – RNA-dependent RNA polymerase

MTase – Methyl transferase

HCV – Hepatitis C virus

Introduction

Kyasanur forest disease (KFD) is an infectious viral hemorrhagic disease primarily infecting human and non-human primates [1]. Mortality in monkeys, especially among the black-faced langurs (*Presbytis entellus*) and red-faced bonnet monkeys (*Macaca radiata*), has been reported during multiple outbreaks of this disease [2]. In addition, birds, squirrels, gerbils, mice, rats, and bats also function as hosts for the virus [3]. The hard-bodied tick, *Haemaphysalis spinigera*, is the primary vector for the Kyasanur forest disease virus (KFDV) [4]. KFDV was also isolated from various genera of ticks, such as *Ixodes, Argas, Ornithodoros, Hyalomma, Dermacentor, and Rhipicephalus* [3]. Clinical symptoms of KFD include

77 high-grade fever, chills, headache, Conjunctivital inflammation,
78 vomiting, abdominal pain, diarrhea, maculopapular eruptions, muscle
79 tenderness, nausea, and persistent cough [5]. In extreme cases,
80 neurological and hemorrhagic manifestations are observed, with an
81 estimated fatality of ~ 3-5% [6]. A microchip-based point-of-care
82 test (Truenat KFD), developed by ICMR-NIV and Molbio Diagnostics,
83 Goa, is currently the gold standard for diagnosis in India [7].
84 Formalin inactivated tissue-culture vaccine is available for KFD,
85 administered in two doses to individuals aged 7–65 years at one-
86 month intervals [8]. However, the immunity conferred by this vaccine
87 is short-lived because of which booster doses are recommended after
88 6–9 months of primary vaccination for five consecutive years [8].
89 Current treatment regimens for KFD are limited to providing
90 symptomatic relief and management [6]. There are no direct-acting
91 antiviral drugs available against KFD. Failure of optimal coverage
92 provided by the vaccine, with the absence of antiviral interventions
93 against KFDV, makes it a public health challenge, necessitating
94 attention toward developing second-generation vaccines and targeted
95 therapies.

96 KFDV is a spherical (~40-65 nm in size) virus containing an
97 icosahedral nucleocapsid enclosing a positive-sense RNA of 10,774
98 bases [9]. Kyasanur forest disease virus genome is closely related
99 to Alkhurma Virus from Saudi Arabia, Omsk hemorrhagic fever virus
100 from Siberia, and Nanjianyin Virus from China [10-12]. The RNA
101 strand codes for a polyprotein comprising three structural (C, E &
102 M) and seven non-structural proteins (NS1, NS2a, 2b, NS3, NS4a, 4b,
103 and NS5 [13]. NS5 belonging to the Flaviviridae family are bi-
104 functional proteins comprising of an N-terminal methyl transferase

105 domain (MTase) and a C-terminal RNA-dependent RNA polymerase domain
106 (RdRp) separated by a linker [14, 15](Fig. 1A). MTase domain
107 methylates N-7 of guanine and 2'-OH ribose of viral RNA cap, in the
108 presence of S-adenosyl methionine as a co-factor. N-7 methylation is
109 critical for enhancing the efficiency of viral translation, and 2'-O
110 methylation is essential for the subversion of the innate immune
111 response during viral infection [15]. RdRp domain of flaviviruses
112 catalyzes the de novo template-dependent formation of phosphodiester
113 bonds in the presence of nucleoside triphosphate (NTP) and divalent
114 metal ions. The canonical structure of the Flaviviridae RdRp domain
115 consists of an encircled right hand containing three subdomains -
116 thumb, palm, and fingers folded, surrounding the active site. RdRps
117 consist of channels, the entry of which is lined with positively
118 charged residues, facilitating NTPs and template RNA entry into the
119 active site [14]. The absence of proofreading exonuclease activity
120 in RdRps may lead to the incorporation of mutations and,
121 consequently, the selection of variants of viruses [16]. Hence, RdRp
122 of NS5 plays a crucial role in viral genome replication and can
123 serve as a potential antiviral drug target [17]. Nucleoside and non-
124 nucleoside inhibitors against NS5 RdRp from different viruses
125 belonging to the Flaviviridae family have been identified [18-25].

126 Sofosbuvir is an FDA-approved drug currently in use for the
127 treatment of Hepatitis C virus (HCV) infection [26, 27]. In this
128 study, we recombinantly expressed KFDV NS5 protein and characterized
129 the purified protein to identify a potential inhibitor of RdRp
130 activity. Sofosbuvir (Pro-drug) and its metabolite were demonstrated
131 to inhibit the RdRp activity of the KFDV NS5 protein.

132

133 **Materials and Methods**

134 **Expression and purification of NS5 from KFDV**

135 Codon-optimized gene corresponding to 5 to 897 amino acids of KFDV
136 NS5 with an N-terminal Hexa-histidine tag was synthesized (Genscript
137 USA) and sub-cloned into pET-28a (+) vector between NdeI and HindIII
138 restriction sites. Transformants of Rosetta2(DE3) pLysS containing
139 pET28a – KFDV NS5 were grown to an OD of 2.0 and induced with 0.5 mM
140 IPTG for 16 hours at 18°C. Induced cells were centrifuged at 5000 g
141 for 10 minutes at 4°C, and the pellet was resuspended in a lysis
142 Buffer containing 20 mM Na_2HPO_4, 0.5 M NaCl, 50 mM L-Arginine, 10 mM
143 $MgSO_4$, 5 mM β-mercaptoethanol, 5 mM Imidazole, 1 mM PMSF, 10%
144 Glycerol, pH 7 [28]. The cell suspension was sonicated, and the
145 lysate was centrifuged at 20000 g for 60 minutes at 4°C. The
146 clarified lysate was filtered with Durapore PVDF 0.22 µm membrane
147 and loaded onto a Ni-NTA affinity column pre-equilibrated with 20 mM
148 Na_2HPO_4, 0.5 M NaCl, 10 % Glycerol pH 7.0. The column was washed with
149 equilibration buffer containing 50 mM Imidazole and bound protein
150 eluted with 20 mM Na_2HPO_4, 0.5 M NaCl, 400 mM Imidazole, 10% Glycerol
151 pH 7.0. Eluates containing a prominent band corresponding to the
152 expected molecular weight of ~104 kDa were injected into Superdex
153 200 Increase 10/300 GL column pre-equilibrated with 50 mM Tris-HCl
154 pH 8.0, 150 mM NaCl, 5 mM $MgCl_2$, 1 mM DTT, 5% Glycerol, 0.05% Tween
155 20. The purified protein was quantified using Bradford assay and
156 densitometry analysis. Purified fractions were transferred onto the
157 PVDF membrane and probed with mouse anti-His primary antibody
158 (1:3000) and anti-mouse IgG HRP—conjugate (1:6000). Gel peptic
159 digest and LC-MS/MS analysis were performed for the gel filtration

160 fractions to ascertain the identity of the NS5 protein.

161

162 **RNA-dependent RNA polymerase activity of purified NS5**

163 RNA-dependent RNA polymerase (RdRp) activity of KFDV NS5 protein was
164 determined by employing a fluorometric endpoint assay based on the
165 intercalating property of a fluorescent dye, SYTO 9, which binds to
166 double-stranded (ds) RNA and not to single-stranded (ss) RNA [29].
167 250 nM of purified NS5 protein was added to a standard reaction mix
168 comprising 50 mM HEPES pH 7.0, 2.5 mM $MnCl_2$, 500 μM ATP, 20 μg/mL
169 poly(U), and 0.1 mg/mL BSA, and the reaction mix was incubated at
170 30°C for 60 minutes in 96 well flat-bottom black plates. The
171 reaction was quenched by adding 25 mM EDTA, following which 0.25 μM
172 SYTO 9 was added and further incubated at room temperature for 7
173 minutes. Fluorescence was recorded in a plate reader (Infinite 200
174 Pro M Plex, TECAN, Switzerland) using excitation and emission
175 filters at 485 nm and 520 nm, respectively. The background
176 fluorescence levels were subtracted from the samples using a protein
177 blank control reaction. The effect of pH, temperature, NaCl, and
178 glycerol concentrations on RdRp activity was determined to identify
179 the optimal conditions using the purified KFDV NS5 protein [30].
180 Buffers with pH ranging from 5.0 to 9.0 (Citrate pH 5.0, Tricine pH
181 6.0, HEPES pH 7.0, Tris-HCl PH 7.5, Tris-HCl pH 8.0, and Bicine pH
182 9.0) were assayed. NS5 protein was incubated at different
183 temperatures of 20°C, 25°C, 30°C, 37°C, and 42°C, different NaCl
184 concentrations (5 mM, 25 mM, 50 mM, 75 mM, 100 mM, 300 mM, and 500
185 mM) and varying percentages of glycerol (5% v/v, 10% v/v, 20% v/v,

186 30% v/v, 40% v/v, 50% v/v). The mean values were computed from the
187 experiments with standard deviation.

188 NS5 protein was titrated against a fixed concentration of 500 µM ATP
189 to arrive at the protein concentration of 250 nM to determine
190 apparent $K_{m,ATP}$. At concentrations ranging from 50 µM to 500 µM, ATP
191 was titrated with 250 nM of purified NS5 protein and 20 µg/mL of
192 poly(U). Mean values were computed with standard deviations (n = 3),
193 and K_m was calculated using GraphPad Prism, 9.3.0.

194 **Determination of inhibitory concentrations for sofosbuvir, its**
195 **metabolite, and dasabuvir**

196 Sofosbuvir, Sofosbuvir triphosphate, and Dasabuvir (MedChemExpress,
197 Monmouth Junction, NJ) were dissolved in DMSO and diluted freshly
198 for the experiment. The inhibitory effect of Sofosbuvir, sofosbuvir
199 triphosphate, and Dasabuvir was determined at different
200 concentrations ranging from 5 µM to 20 µM. The assay was performed
201 in presence of 250 nM of NS5 protein, 20 µg/mL poly(U) and 500 µM
202 ATP in the reaction buffer containing 50 mM HEPES pH 7.0, 5 mM NaCl,
203 10% glycerol, 0.1 mg/ml BSA. IC_{50} values were determined using a non-
204 linear regression model with GraphPad Prism, 9.3.0. The mean values
205 were computed with standard deviation (n = 3).

206

207 **Results**

208 **KFDV NS5 was expressed in bacteria and purified with affinity column**
209 **and size exclusion chromatography**

210 Multiple sequence alignment of KFDV polyprotein (Uniprot id: D7RF80)
211 with NS5 proteins from tick-borne encephalitis virus (TBEV), Yellow

212 fever virus (YEFV), Zika virus (ZKV), Japanese encephalitis virus
213 (JAEV), West Nile virus (WNV) and Dengue virus serotype 2 (DENV2),
214 led to the identification of KFDV NS5 protein, i.e., between amino
215 acids, 2514 to 3416 in the polyprotein sequence. NS5 protein is
216 widely conserved across the Flaviviridae family (50 – 70%
217 identity/similarity). Residues 5 to 897 of NS5 protein containing
218 the MTase and RdRp domain (Fig. 1A) were expressed with an N-
219 terminal Hexa histidine tag in bacteria and purified with Ni-NTA
220 affinity chromatography (Fig. 1B). A lower molecular weight
221 contaminant band (Fig. 1) was observed along with the band
222 corresponding to the expected molecular weight of NS5 (~104 kDa), on
223 the Coomassie blue stained SDS-PAGE gel. Anti-His antibody also
224 recognized the lower molecular weight contaminant band with western
225 blotting, suggesting it to be an N-terminal degradation product. It
226 was confirmed with amino acid sequencing of tryptic digests with LC-
227 MS/MS. The sequence corresponded to 5 to 282 amino acids of the NS5
228 protein (Data not shown). This histidine-tagged N-terminal fragment
229 co-eluting with NS5 protein in affinity chromatography was removed
230 with superdex 200 increase 10/300 GL size exclusion column
231 chromatography (Peak P2 from Fig. 1C) to the extent that it was not
232 observed in a Coomassie-stained SDS-PAGE gel. The identity of the
233 NS5 protein - Peak, P1 corresponding to the expected molecular
234 weight of 104 kDa, was confirmed with LC-MS/MS analysis and western
235 blot analysis using an anti-His antibody (Fig. 1D). The yield of NS5
236 protein after size exclusion chromatography (P1 fraction) was 1
237 mg/liter of bacterial culture.

238 **Apparent $K_{m,ATP}$ for NS5 RDRP from KFDV is comparable to that**
239 **determined for other viruses**

240 KFDV NS5 construct containing both the MTase and RdRp domains was
241 used in this study to rule out any effect of the MTase domain on
242 RdRp activity. The interplay of both the RdRp and MT domains was
243 earlier demonstrated for Dengue and Zika NS5 [31-33]. Compared to 5%
244 glycerol, KFDV NS5 showed an increase in RdRp activity at 10%
245 glycerol, which significantly reduced at 20% (Fig 2). Inhibition of
246 RdRp activity of KFDV NS5 was observed at lower concentration ranges
247 of NaCl consistent with an earlier report from Usutu virus NS5 [30].
248 RdRp from HCV tolerated NaCl concentrations until 100 mM without
249 significant RdRp activity loss [34]. However, it is unclear how
250 Dengue and KFDV/Usutu NS5 proteins differ in their sensitivity to
251 different concentrations of NaCl. Mechanistically, the binding of
252 Dengue NS5 to ssRNA has been shown to release six Na^+ ions [35].
253 Based on this report, the loss of activity can be speculated to be
254 due to the dissociation of RNA at higher concentrations of NaCl and
255 not due to the denaturation of protein. At a pH of 7.0, maximal
256 activity was observed, tapered at pHs 5.0 and 9.0. The optimal
257 activity was observed at a temperature of 30°C at pH 7, without
258 significant activity loss at 42°C (Fig 2). Apparent $K_{m,ATP}$ was
259 determined to be 42.15 $\pm$ 5.81 μM for KFDV NS5, under the tested
260 conditions, as described in methods (Fig. 3). The reported values of
261 $k_{m,GTP}$ for glutathionylated Dengue and Zika NS5 were 189.8 $\pm$ 52.5 μM,
262 and 137.2 $\pm$ 41.3 μM, respectively [36]. Motif F from the ring domain
263 of RdRp with highly conserved Lys, Glu, Arg residues, and motif G
264 from pinky finger domain, with conserved ala, binds to NTPs, and
265 +1/+2 junction of the template strand, respectively (Fig. 4) [37].
266 The comparable values of apparent $K_{m,ATP}$ to $K_{m,GTP}$ validates the use of
267 the purified protein for inhibition studies.

268 **Sofosbuvir and sofosbuvir triphosphate inhibit the RDRP activity of**
269 **KFDV NS5.**

270 With HCV NS5, the half-maximal inhibitory concentrations of
271 sofosbuvir triphosphate and sofosbuvir were reported to be 0.12 µM
272 and 2.06 ug/mL (corresponding to 3.8905 µM), respectively (24, 57).
273 X-ray crystal structure of HCV NS5B with sofosbuvir (PDB: 4WTG)
274 showed a critical interaction of Asn291 with the 2'-F group of
275 Sofosbuvir, leading to its incorporation into the growing RNA chain
276 and, subsequently, chain termination (Fig. 4) [39]. As indicated
277 earlier, active site residues in the Flaviviridae family are highly
278 conserved, including Asn291 increasing the likelihood of Sofosbuvir
279 inhibiting KFDV NS5. Sofosbuvir and sofosbuvir triphosphate
280 exhibited IC_{50} of 3.45 ± 0.012 and 3.73 ± 0.033 µM, respectively
281 against KFDV NS5 (Fig. 5). Interestingly, Dasabuvir, a nonnucleoside
282 analog, did not show inhibition of RdRp activity, even at 100 µM,
283 under the tested conditions. IC_{50} of Dasabuvir varied between
284 nanomolar and micromolar concentrations when tested against
285 different genotypes of HCV RdRps [25]. Also, Dasabuvir is not
286 predicted to bind to conserved residues in RdRps across other
287 viruses [40].

288

289 **Discussion**

290 Kyasanur forest disease virus is a high-risk category pathogen
291 endemic to southern India. The current line of treatment for KFD
292 includes maintaining hydration, blood work, and management of
293 neurological and hemorrhagic conditions [5,6]. Sofosbuvir, also
294 known as L-Alanine, N-[[P(S),2'R]-2'-deoxy-2'-fluoro-2'-methyl-P-

295 phenyl-5′-uridylyl]-,1-methyl ethyl ester ($C_{22}H_{29}FN_3O_9P$), is an orally
296 available nucleotide analog, approved for the treatment of HCV viral
297 infections [26]. In preclinical studies, Sofosbuvir has exhibited
298 inhibitory activity against all genotypes of HCV [41]. Sofosbuvir
299 has been indicated for chronic HCV infection (genotype 1, 2, 3, or
300 4) in adults as part of combination therapy and in children older
301 than 3 years with genotype for chronic HCV infections with
302 ribavirin. Many Clinical trials are ongoing for evaluating
303 sofosbuvir in different populations and dosing regimens in
304 combination with other drugs against HCV [42 – 46]. Sofosbuvir also
305 exhibited inhibitory activity against Dengue, Chikungunya, Yellow
306 fever virus, Hepatitis E virus, and SARS-CoV2 [47 -51]. Sofosbuvir
307 (PSI-7977) is metabolized to its triphosphate metabolite, β-D-2'-
308 deoxy-2'-fluoro-2'-C-methyluridine 5'-triphosphate (PSI-7409), by
309 hydrolysis of the carboxyl ester moiety, spontaneous release of the
310 Phenyl group, deamidation and phosphorylation [52, 53]. KFDV NS5
311 expression construct used in this study also included the MTase
312 domain, as the MTase was demonstrated to influence the activity RdRp
313 domain by interaction with the template RNA [38]. KFDV NS5 protein
314 was recombinantly expressed in bacteria, and so were NS5 proteins
315 from Usutu, Zika, Japanese encephalitis, Dengue, HCV, and West Nile
316 virus [30, 33, 37, 54, 55, 56]. Recombinantly purified NS5 RDRP
317 protein from the Zika virus exhibited an IC_{50} of 0.38 ± 0.03 μM
318 against sofosbuvir triphosphate [56, 47]. The inhibitory
319 concentration (IC_{50}) of sofosbuvir triphosphate and sofosbuvir were
320 in the same range for KFDV NS5. This could be due to differences in
321 the architecture of sofosbuvir binding sites across viruses.
322 This is the first report on the expression and purification of the

NS5 protein of KFDV, its assay establishment, and the demonstration of inhibition of RdRp activity by sofosbuvir. Further, the established biochemical assay can screen potential inhibitors of KFDV RdRp. Drug repurposing approaches against KFD, a neglected disease, can pave the way for identifying novel inhibitors for developing targeted therapeutic interventions against the disease.

Acknowledgments

The authors thank Tata Trusts for funding this study. We would like to acknowledge the NCBS-inStem-CCAMP mass spectrometry facility for the technical assistance provided for this study.

Conflict of interest

The authors declare no conflict of interest.

Availability of data and materials

All the relevant data used to support the findings of this study are included in the article.

References

[1] T.H. Work, H. Trapido, D.P. Narasimha Murthy, R. Laxmana Rao, P.N. Bhatt, K.G. Kul-karni, Kyasanur Forest Disease III. A Preliminary Report on the Nature of the Infection and Clinical

Manifestations in Human Beings., Indian J. Med. Sci. 11 (1957) 619–45.

[2] K. V. Shah, C.N. Dandawate, P.N. Bhatt, Kyasanur forest disease virus: viremia and challenge studies in monkeys with evidence of cross-protection by Langat virus infection, F1000Research. 1 (2012). https://doi.org/10.12688/F1000RESEARCH.1-61.V1.

[3] K. Muraleedharan, Wildlife Arthropods of Karnataka with Special Reference to KFD Endemic Area of Shivamogga District: Those Parasitic on Small and Large Mammals, (2016). www.jakraya.com/journal/vri.

[4] M.G.R. Varma, H.E. Webb, K.M. Pavri, Studies on the transmission of Kyasanur Forest disease virus by Haemaphysalis spinigera newman, Trans. R. Soc. Trop. Med. Hyg. 54 (1960) 509–516. https://doi.org/10.1016/0035-9203(60)90024-9.

[5] A. Munivenkatappa, R.R. Sahay, P.D. Yadav, R. Viswanathan, D.T. Mourya, Clinical & epidemiological significance of Kyasanur forest disease, Indian J. Med. Res. 148 (2018) 145. https://doi.org/10.4103/IJMR.IJMR_688_17.

[6] Kyasanur forest disease, Centers for Disease Control and Prevention, National Center for Emerging and Zoonotic Infectious Diseases (NCEZID), Division of High-Consequence Pathogens and Pathology (DHCPP), Viral Special Pathogens Branch (VSPB). https://www.cdc.gov/vhf/kyasanur/index.html

[7] T. Majumdar, A. Shete, P. Yadav, S. Patil, D. Mali, A. Waghmare, P. Gawande, Point of care real-time polymerase chain

372 reaction-based diagnostic for Kyasanur forest disease, Int. J.
373 Infect. Dis. 108 (2021) 226–230.
374 https://doi.org/10.1016/J.IJID.2021.05.036.

375 [8] G.S. Kasabi, M. V. Murhekar, V.K. Sandhya, R. Raghunandan,
376 S.K. Kiran, G.H. Channabasappa, S.M. Mehendale, Coverage and
377 Effectiveness of Kyasanur Forest Disease (KFD) Vaccine in Karnataka,
378 South India, 2005–10, PLoS Negl. Trop. Dis. 7 (2013) e2025.
379 https://doi.org/10.1371/JOURNAL.PNTD.0002025.

380 [9] K.A. Dodd, B.H. Bird, M.L. Khristova, C.G. Albariño, S.A.
381 Carroll, J.A. Comer, B.R. Erickson, P.E. Rollin, S.T. Nichol,
382 Ancient Ancestry of KFDV and AHFV Revealed by Complete Genome
383 Analyses of Viruses Isolated from Ticks and Mammalian Hosts, PLoS
384 Negl. Trop. Dis. 5 (2011) e1352.
385 https://doi.org/10.1371/JOURNAL.PNTD.0001352.

386 [10] B. Bhatia, H. Feldmann, A. Marzi, Kyasanur Forest Disease and
387 Alkhurma Hemorrhagic Fever Virus—Two Neglected Zoonotic Pathogens,
388 Microorg. 2020, Vol. 8, Page 1406. 8 (2020) 1406.
389 https://doi.org/10.3390/MICROORGANISMS8091406.

390 [11] D. Lin, L. Li, D. Dick, R.E. Shope, H. Feldmann, A.D.T.
391 Barrett, M.R. Holbrook, Analysis of the complete genome of the tick-
392 borne flavivirus Omsk hemorrhagic fever virus, Virology. 313 (2003)
393 81–90. https://doi.org/10.1016/S0042-6822(03)00246-0.

394 [12] J. Wang, H. Zhang, S. Fu, H. Wang, D. Ni, R. Nasci, Q. Tang,
395 G. Liang, Isolation of Kyasanur Forest Disease Virus from Febrile
396 Patient, Yunnan, China, Emerg. Infect. Dis. 15 (2009) 326.
397 https://doi.org/10.3201/EID1502.080979.

398 [13] K. Venugopal, T. Gritsun, V.A. Lashkevich, E.A. Gould,
399 Analysis of the structural protein gene sequence shows Kyasanur
400 Forest disease virus as a distinct member in the tick-borne
401 encephalitis virus serocomplex, J. Gen. Virol. 75 (1994) 227–232.
402 https://doi.org/10.1099/0022-1317-75-1-227.

403 [14] J. Wu, W. Liu, P. Gong, P. Gong, A Structural Overview of RNA-
404 Dependent RNA Polymerases from the Flaviviridae Family, Int. J. Mol.
405 Sci. 2015, Vol. 16, Pages 12943-12957. 16 (2015) 12943–12957.
406 https://doi.org/10.3390/IJMS160612943.

407 [15] H. Dong, K. Fink, R. Züst, S.P. Lim, C.F. Qin, P.Y. Shi,
408 Flavivirus RNA methylation, J. Gen. Virol. 95 (2014) 763–778.
409 https://doi.org/10.1099/VIR.0.062208-0/CITE/REFWORKS.

410 [16] S.F. Elena, R. Sanjuán, Adaptive Value of High Mutation Rates
411 of RNA Viruses: Separating Causes from Consequences, J. Virol. 79
412 (2005) 11555–11558. https://doi.org/10.1128/JVI.79.18.11555-
413 11558.2005.

414 [17] P.O. Fernandes, M.A. Chagas, W.R. Rocha, A.H. Moraes, Non-
415 structural protein 5 (NS5) as a target for antiviral development
416 against established and emergent flaviviruses, Curr. Opin. Virol. 50
417 (2021) 30–39. https://doi.org/10.1016/J.COVIRO.2021.07.001.

418 [18] X. Yao, S. Guo, W. Wu, J. Wang, S. Wu, S. He, Y. Wan, K.S.
419 Nandakumar, X. Chen, N. Sun, Q. Zhu, S. Liu, Q63, a novel DENV2 RdRp
420 non-nucleoside inhibitor, inhibited DENV2 replication and infection,
421 J. Pharmacol. Sci. 138 (2018) 247–256.
422 https://doi.org/10.1016/J.JPHS.2018.06.012.

423 [19] R. Arora, C.W. Liew, T.S. Soh, D.A. Otoo, C.C. Seh, K. Yue, S.
424 Nilar, G. Wang, F. Yokokawa, C.G. Noble, Y.L. Chen, P.-Y. Shi, J.
425 Lescar, T.M. Smith, T.E. Benson, S.P. Lim, Two RNA Tunnel Inhibitors
426 Bind in Highly Conserved Sites in Dengue Virus NS5 Polymerase:
427 Structural and Functional Studies, J. Virol. 94 (2020).
428 https://doi.org/10.1128/JVI.01130-20

429 [20] Y. Chen, Z. Li, P. Pan, Z. Lao, J. Xu, Z. Li, S. Zhan, X. Liu,
430 Y. Wu, W. Wang, G. Li, Cinnamic acid inhibits Zika virus by
431 inhibiting RdRp activity, Antiviral Res. 192 (2021) 105117.
432 https://doi.org/10.1016/J.ANTIVIRAL.2021.105117.

433

434 [21] Y. Lin, H. Zhang, W. Song, S. Si, Y. Han, J. Jiang,
435 Identification and characterization of Zika virus NS5 RNA-dependent
436 RNA polymerase inhibitors, Int. J. Antimicrob. Agents. 54 (2019)
437 502–506. https://doi.org/10.1016/J.IJANTIMICAG.2019.07.010.

438 [22] P. Coulerie, M. Nour, A. Maciuk, C. Eydoux, J.C. Guillemot, N.
439 Lebouvier, E. Hnawia, K. Leblanc, G. Lewin, B. Canard, B. Figadère,
440 Structure-Activity Relationship Study of Biflavonoids on the Dengue
441 Virus Polymerase DENV-NS5 RdRp, Planta Med. 79 (2013) 1313–1318.
442 https://doi.org/10.1055/S-0033-1350672.

443 [23] M.A. Abu-Zaied, S.F. Hammad, F.T. Halaweish, G.H. Elgemeie,
444 Sofosbuvir Thio-analogues: Synthesis and Antiviral Evaluation of the
445 First Novel Pyridine- And Pyrimidine-Based Thioglycoside
446 Phosphoramidates, ACS Omega. 5 (2020) 14645–14655.
447 https://doi.org/10.1021/ACSOMEGA.0C01364

448 [24] Fenaux, M., Lin, X., Yokokawa, F., Sweeney, Z., Saunders, O.,
449 Xie, L., ... & Zhong, W. (2016). Antiviral nucleotide incorporation
450 by recombinant human mitochondrial RNA polymerase is predictive of
451 increased in vivo mitochondrial toxicity risk. Antimicrobial agents
452 and chemotherapy, 60(12), 7077-7085.

453 [25] W. Kati, G. Koev, M. Irvin, J. Beyer, Y. Liu, P. Krishnan, T.
454 Reisch, R. Mondal, R. Wagner, A. Molla, C. Maring, C. Collins, In
455 vitro activity and resistance profile of dasabuvir, a nonnucleoside
456 hepatitis c virus polymerase inhibitor, Antimicrob. Agents
457 Chemother. 59 (2015) 1505–1511. https://doi.org/10.1128/AAC.04619-
458 14.

459 [26] I. Gentile, F. Borgia, A. R. Buonomo, G. Castaldo, G. Borgia,
460 A Novel Promising Therapeutic Option Against Hepatitis C Virus: An
461 Oral Nucleotide NS5B Polymerase Inhibitor Sofosbuvir, Curr Med Chem
462 20(30) 3733-3742. https://doi.org/10.2174/09298673113209990178.

463 [27] E. Lawitz, I.M. Jacobson, D.R. Nelson, S. Zeuzem, M.S.
464 Sulkowski, R. Esteban, D. Brainard, J. Mcnally, W.T. Symonds, J.G.
465 Mchutchison, D. Dieterich, E. Gane, Development of sofosbuvir for
466 the treatment of hepatitis C virus infection, Ann. N. Y. Acad. Sci.
467 1358 (2015) 56–67. https://doi.org/10.1111/NYAS.12832.

468 [28] R.P. Dos Santos Alves, L.R. Pereira, D.L.N. Fabris, F.S.
469 Salvador, R.A. Santos, P.M. De Andrade Zanotto, C.M. Romano, J.H.
470 Amorim, L.C. De Souza Ferreira, Production of a recombinant dengue
471 virus 2 NS5 protein and potential use as a vaccine antigen, Clin.
472 Vaccine Immunol. 23 (2016) 460–469.
473 https://doi.org/10.1128/CVI.00081-16.

474 [29] Y. Sáez-Álvarez, A. Arias, C. del Águila, R. Agudo,
475 Development of a fluorescence-based method for the rapid
476 determination of Zika virus polymerase activity and the screening of
477 antiviral drugs, Sci. Reports 2019 91. 9 (2019) 1–11.
478 https://doi.org/10.1038/s41598-019-41998-1.

479 [30] L. Albentosa-González, P. Clemente-Casares, R. Sabariegos, A.
480 Mas, Polymerase activity, protein-protein interaction, and cellular
481 localization of the Usutu virus NS5 protein, Antimicrob. Agents
482 Chemother. 64 (2020). https://doi.org/10.1128/AAC.01573-19.

483 [31] Y. Zhao, T.S. Soh, J. Zheng, K.W.K. Chan, W.W. Phoo, C.C. Lee,
484 M.Y.F. Tay, K. Swaminathan, T.C. Cornvik, S.P. Lim, P.Y. Shi, J.
485 Lescar, S.G. Vasudevan, D. Luo, A Crystal Structure of the Dengue
486 Virus NS5 Protein Reveals a Novel Inter-domain Interface Essential
487 for Protein Flexibility and Virus Replication, PLOS Pathog. 11
488 (2015) e1004682. https://doi.org/10.1371/JOURNAL.PPAT.1004682.

489 [32] S.P. Lim, J.H.K. Koh, C.C. Seh, C.W. Liew, A.D. Davidson, L.S.
490 Chua, R. Chandrasekaran, T.C. Cornvik, P.Y. Shi, J. Lescar, A
491 crystal structure of the dengue virus non-structural protein 5 (NS5)
492 polymerase delineates interdomain amino acid residues that enhance
493 its thermostability and de novo initiation activities, J. Biol.
494 Chem. 288 (2013) 31105–31114.
495 https://doi.org/10.1074/jbc.M113.508606.

496 [33] B. Zhao, G. Yi, F. Du, Y. C. Chuang, R. C. Vaughan, B.
497 Sankaran, et al., Structure and function of the Zika virus full-
498 length NS5 protein, Nat. Commun. 8 (2017) 14762.
499 https://doi:10.1038/ncomms14762.

500 [34] V. Lohmann, A. Roos, F. Körner, J.O. Koch, R. Bartenschlager,
501 Biochemical and Kinetic Analyses of NS5B RNA-Dependent RNA
502 Polymerase of the Hepatitis C Virus, Virology. 249 (1998) 108–118.
503 https://doi.org/10.1006/VIRO.1998.9311.

504 [35] M.R. Szymanski, M.J. Jezewska, P.J. Bujalowski, C. Bussetta,
505 M. Ye, K.H. Choi, W. Bujalowski, Full-length Dengue Virus RNA-
506 dependent RNA Polymerase-RNA/DNA Complexes, J. Biol. Chem. 286
507 (2011) 33095–33108. https://doi.org/10.1074/jbc.m111.255034.

508 [36] C. Saisawang, A. Kuadkitkan, P. Auewarakul, D.R. Smith, A.J.
509 Ketterman, Glutathionylation of dengue and Zika NS5 proteins affects
510 guanylyltransferase and RNA dependent RNA polymerase activities,
511 PLoS One. 13 (2018) e0193133.
512 https://doi.org/10.1371/JOURNAL.PONE.0193133.

513 [37] G. Lu, P. Gong, Crystal Structure of the Full-Length
514 Japanese Encephalitis Virus NS5 Reveals a Conserved
515 Methyltransferase-Polymerase Interface, PLOS Pathog. 9 (2013)
516 e1003549. https://doi.org/10.1371/JOURNAL.PPAT.1003549.

517 [38] T. Rusanov, T. Kent, M. Saeed, T.M. Hoang, C. Thomas, C.M.
518 Rice, R.T. Pomerantz, Identification of a Small Interface between
519 the Methyltransferase and RNA Polymerase of NS5 that is Essential
520 for Zika Virus Replication, Sci. Reports 2018 81. 8 (2018) 1–11.
521 https://doi.org/10.1038/s41598-018-35511-3.

522 [39] T.C. Appleby, J.K. Perry, E. Murakami, O. Barauskas, J. Feng,
523 A. Cho, D. Fox, D.R. Wetmore, M.E. McGrath, A.S. Ray, M.J. Sofia, S.
524 Swaminathan, T.E. Edwards, Structural basis for RNA replication by

525 the hepatitis C virus polymerase, Science (80-.). 347 (2015) 771–
526 775. https://doi.org/10.1126/SCIENCE.1259210.

527 [40] P.P.L.F. de Albuquerque, L.H.S. Santos, D. Antunes, E.R.
528 Caffarena, A.S. Figueiredo, Structural insights into NS5B protein of
529 novel equine hepaciviruses and pegiviruses complexed with polymerase
530 inhibitors, Virus Res. 278 (2020) 197867.
531 https://doi.org/10.1016/J.VIRUSRES.2020.197867.

532 [41] B. Han, R. Martin, S. Xu, A. Parvangada, E.S. Svarovskaia, H.
533 Mo, H. Dvory-Sobol, Sofosbuvir susceptibility of genotype 1 to 6 HCV
534 from DAA-naïve subjects, Antiviral Res. 170 (2019) 104574.
535 https://doi.org/10.1016/J.ANTIVIRAL.2019.104574.

536 [42] A.S. Price, A.K. Nelson, A. Ghosh, S. Kottilil, J. V. Chua, A
537 Phase 2 open label study of ledipasvir/sofosbuvir for 12 weeks in
538 subjects with hepatitis B virus infection, J. Med. Virol. (2022).
539 https://doi.org/10.1002/JMV.28105.

540 [43] V. Virlogeux, L. Choupeaux, P. Pradat, M. Maynard, F. Bailly,
541 C. Scholtès, M.C. Gagnieu, F. Zoulim, Sofosbuvir plus daclatasvir
542 with or without ribavirin for chronic hepatitis C infection: Impact
543 of drug concentration on viral load decay, Dig. Liver Dis. 48 (2016)
544 1351–1356. https://doi.org/10.1016/J.DLD.2016.07.014.

545 [44] M. H. El-Sayed, Clinical Pharmacokinetics of
546 Daclatasvir/Sofosbuvir in Adolescents with Hepatitis C Virus.
547 ClinicalTrials.gov. https://clinicaltrials.gov/ct2/show/NCT03540212.

548 [45] A. A. A. Elmoety, Evaluation of Sofosbuvir and Daclatasvir
549 Combo in COIVD-19 Patients in Egypt. ClinicalTrials.gov.
550 https://www.clinicaltrials.gov/ct2/show/NCT04773756.

551 [46] C. Chappell, Safety, Tolerability, and Outcomes of
552 Velpatasvir/SofosbuviR in Treatment of Chronic Hepatitis C Virus
553 During Pregnancy (STORC). Clinicaltrials.gov.
554 https://clinicaltrials.gov/ct2/show/NCT05140941.

555 [47] H.T. Xu, S.P. Colby-Germinario, S.A. Hassounah, C. Fogarty, N.
556 Osman, N. Palanisamy, Y. Han, M. Oliveira, Y. Quan, M.A. Wainberg,
557 Evaluation of Sofosbuvir (β-D-2′-deoxy-2′-α-fluoro-2′-β-C-
558 methyluridine) as an inhibitor of Dengue virus replication, Sci.
559 Reports 2017 71. 7 (2017) 1–11. https://doi.org/10.1038/s41598-017-
560 06612-2.

561 [48] A.C. Ferreira, P.A. Reis, C.S. de Freitas, C.Q. Sacramento,
562 L.V.B. Hoelz, M.M. Bastos, M. Mattos, N. Rocha, I.G. de Azevedo
563 Quintanilha, C. da Silva Gouveia Pedrosa, L.R.Q. Souza, E.C. Loiola,
564 P. Trindade, Y.R. Vieira, G. Barbosa-Lima, H.C. de Castro Faria
565 Neto, N. Boechat, S.K. Rehen, K. Brüning, F.A. Bozza, P.T. Bozza,
566 T.M.L. Souza, Beyond members of the Flaviviridae family, sofosbuvir
567 also inhibits chikungunya virus replication, Antimicrob. Agents
568 Chemother. 63 (2019). https://doi.org/10.1128/AAC.01389-18.

569 [49] C.S. de Freitas, L.M. Higa, C.Q. Sacramento, A.C. Ferreira,
570 P.A. Reis, et al, Yellow fever virus is susceptible to sofosbuvir
571 both in vitro and in vivo, PLoS Negl. Trop. Dis. 13 (2019) e0007072.
572 https://doi.org/10.1371/JOURNAL.PNTD.0007072.

573 [50] Z. Liang, J. Shu, Q. He, F. Zhang, L. Dai, L. Wang, F. Lu, L.
574 Wang, High dose sofosbuvir and sofosbuvir-plus-ribavirin therapy
575 inhibit Hepatitis E Virus (HEV) replication in a rabbit model for
576 acute HEV infection, Antiviral Res. 199 (2022) 105274.
577 https://doi.org/10.1016/J.ANTIVIRAL.2022.105274.

578 [51] C.Q. Sacramento, N. Fintelman-Rodrigues, J.R. Temerozo,
579 A.D.P.D. Da Silva, S.D.S.G. Dias, et al, In vitro antiviral activity
580 of the anti-HCV drugs daclatasvir and sofosbuvir against SARS-CoV-2,
581 the aetiological agent of COVID-19, J. Antimicrob. Chemother. 76
582 (2021) 1874–1885. https://doi.org/10.1093/JAC/DKAB072.

583 [52] E. Murakami, T. Tolstykh, H. Bao, C. Niu, H.M. Micolochick
584 Steuer, D. Bao, W. Chang, C. Espiritu, S. Bansal, A.M. Lam, M.J.
585 Otto, M.J. Sofia, P.A. Furman, Mechanism of activation of PSI-7851
586 and its diastereoisomer PSI-7977, J. Biol. Chem. 285 (2010) 34337–
587 34347. https://doi.org/10.1074/jbc.M110.161802.

588 [53] S. Chen, J. Wu, X. Yang, Q. Sun, S. Liu, F. Rashid, E.E.
589 Dzakah, H. Wang, J. Wang, P. Gong, S. Tang, RNA-Dependent RNA
590 Polymerase of the Second Human Pegivirus Exhibits a High-Fidelity
591 Feature, Microbiol. Spectr. (2022).
592 https://doi.org/10.1128/SPECTRUM.02729-22.

593 [54] T. Rusanov, T. Kent, M. Saeed, T.M. Hoang, C. Thomas, C.M.
594 Rice, R.T. Pomerantz, Identification of a Small Interface between
595 the Methyltransferase and RNA Polymerase of NS5 that is Essential
596 for Zika Virus Replication, Sci. Reports 2018 81. 8 (2018) 1–11.
597 https://doi.org/10.1038/s41598-018-35511-3

598 [55] J.-W. Oh, T. Ito, M.M.C. Lai, A Recombinant Hepatitis C
599 Virus RNA-Dependent RNA Polymerase Capable of Copying the Full-
600 Length Viral RNA, J. Virol. 73 (1999) 7694–7702.
601 https://doi.org/10.1128/JVI.73.9.7694-7702.1999.

602 [56] Sacramento, C. Q., de Melo, G. R., de Freitas, C. S., Rocha,
603 N., Hoelz, L. V. B., Miranda, M., ... & Souza, T. M. L. (2017). The

604 clinically approved antiviral drug sofosbuvir inhibits Zika virus
605 replication. Scientific reports, 7(1), 1-12.

606 57. Abu-Zaied, M. A., Hammad, S. F., Halaweish, F. T., & Elgemeie,
607 G. H. (2020). Sofosbuvir Thio-analogues: Synthesis and Antiviral
608 Evaluation of the First Novel Pyridine-and Pyrimidine-Based
609 Thioglycoside Phosphoramidates. ACS omega, 5(24), 14645-14655.

610

611 **Figure Legends**

612 Fig. 1. NS5 protein of Kyasanur forest disease virus. A. Schematic
613 representation of NS5 protein domains - N-terminal methyl
614 transferase (MTase – 1 to 263) and C-terminal RNA dependent RNA
615 polymerase (RdRp – 274 to 903). Linker (L – 264 to 273 amino acids)
616 residues connecting the two domains are not conserved among
617 flaviviruses (35). B. Coomassie-stained SDS-PAGE gel (12%)
618 containing Ni-NTA affinity column elutes. Lanes containing a
619 prominent band of the expected molecular weight of 104 kDa,
620 corresponding to 5 to 897 amino acids of NS5, are seen in the elutes
621 (indicated by an arrow). Also seen is a lower molecular weight band
622 between the molecular weight markers - 35 kDa and 25 kDa (*). C.
623 Superdex increase 200 10/300 GL fractionation of affinity purified
624 fraction of NS5 protein. Peaks P1 and P2 correspond to NS5 and the
625 lower molecular weight protein (*). Coomassie-stained SDS-PAGE gel
626 is on the left panel. D. anti- Histidine tagged antibody probed
627 western blot of P1 and P2 fractions. The prominent bands in P1 (NS5
628 protein indicated with arrowhead) and P2 (lower molecular weight
629 contaminant band marked with asterisks) were recognized by an anti-
630 His antibody.

631

632 Fig. 2. Optimization of reaction conditions for RdRp activity of
633 KFDV NS5. Effect of pH (A), NaCl (B), glycerol (C), and temperature
634 (D) on RdRp activity. Activity is represented as arbitrary
635 fluorescence units (A.U.) on the Y-axis. For every sample well,
636 fluorescence units were subtracted from a blank control devoid of
637 NS5 protein under the same conditions. The standard deviation was
638 computed and represented as error bars for every data point.

639

640 Fig. 3. Determination of apparent $K_{m,ATP}$ for RdRp domain of KFDV NS5.
641 Apparent K_m for ATP was determined by Michaelis-Menten equation
642 using graph pad prism 9.3.0. The representative graph contains
643 values averaged from at least three independent experiments (n=3).
644 Activity is represented as arbitrary fluorescence units (A.U.) on
645 the Y-axis. The standard deviation error bars are shown for every
646 data point.

647

648 Fig. 4. Amino acid sequence alignment of motifs F, G, and B of NS5
649 from the Flaviviridae family. Kyasanur forest disease virus (KFDV),
650 Alkhurma hemorrhagic fever (ALKV), Tick-borne encephalitis virus
651 (TBEV), Yellow fever virus (YEFV), Zika virus (ZKV), Japanese
652 encephalitis virus (JAEV), West Nile virus (WNV) Dengue virus
653 serotype 2 (DENV2), Hepatitis C virus (HCV). Conserved residues in
654 Motif F and motif G, from ring and pinky finger domains involved in
655 interacting with NTPs and the template, respectively, are
656 highlighted. Asn291 from the NS5 RdRp domain of HCV makes a critical

interaction with Sofosbuvir [33]. Asn291 is highly conserved across the sequences shown in the figure (marked as *). There is a higher level of conservation among the flavivirus genus than flaviviruses and HCV (which belong to the genus Hepacivirus).

Fig. 5. Determination of IC_{50} for sofosbuvir (A) and sofosbuvir triphosphate (B). Increasing concentrations of Sofosbuvir and sofosbuvir triphosphate were titrated using the optimized assay conditions described in the methods. The log of compound concentration is plotted against percentage activity and IC_{50}, computed from the profiles using Graph pad prism 9.3.0 (n=3). The structures of compounds are shown above the IC_{50} graphs.

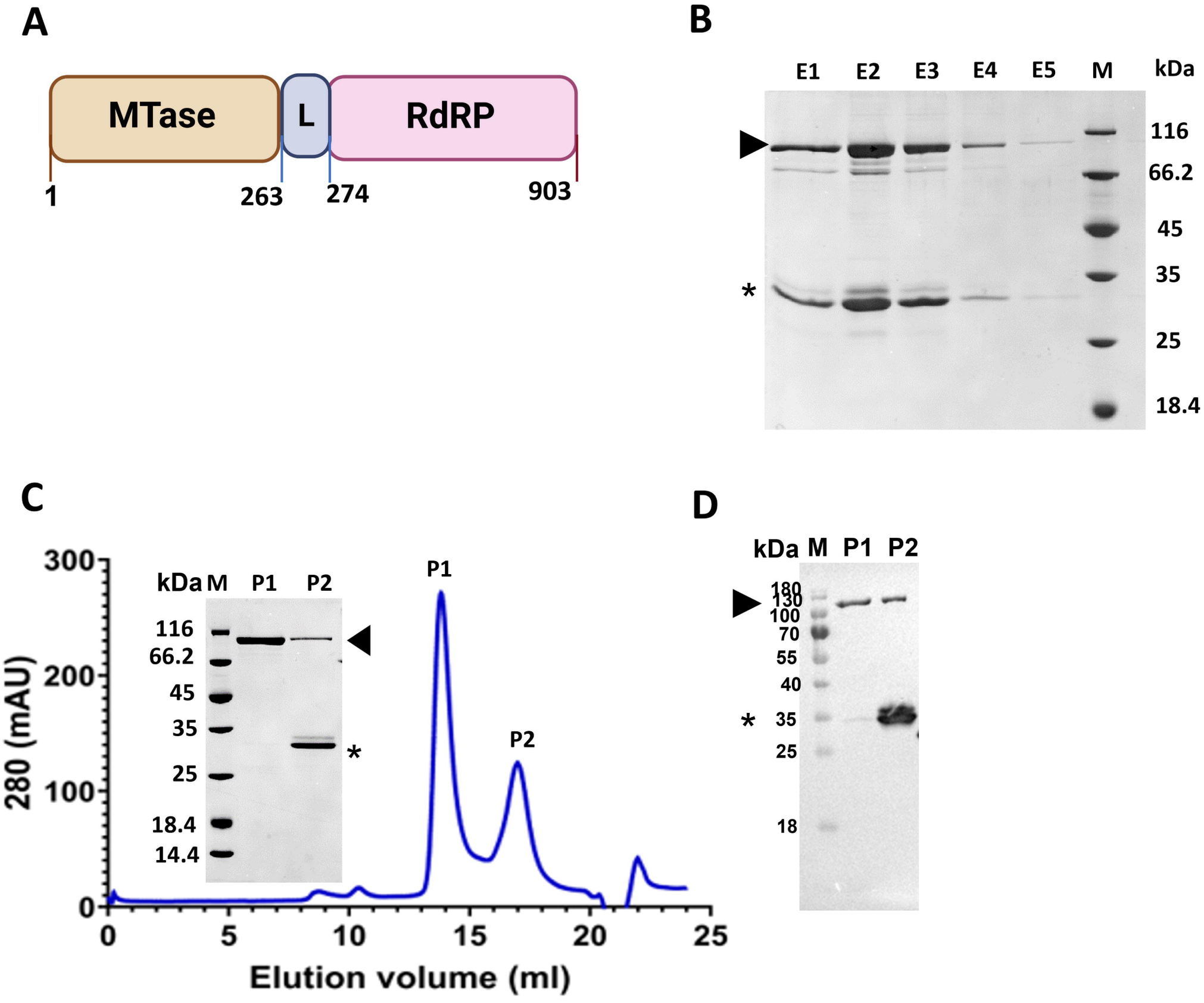
A
MTase
L
RdRP
1
263
274
903
B
E1
E2
E3
E4
E5
M
kDa
116
66.2
45
35
25
18.4
*
C
kDa M P1 P2
116
66.2
45
35
25
18.4
14.4
*
P1
P2
280 (mAU)
300
200
100
0
0
5
10
15
20
25
Elution volume (ml)
D
kDa M P1 P2
180
130
100
70
55
40
35
25
18
*

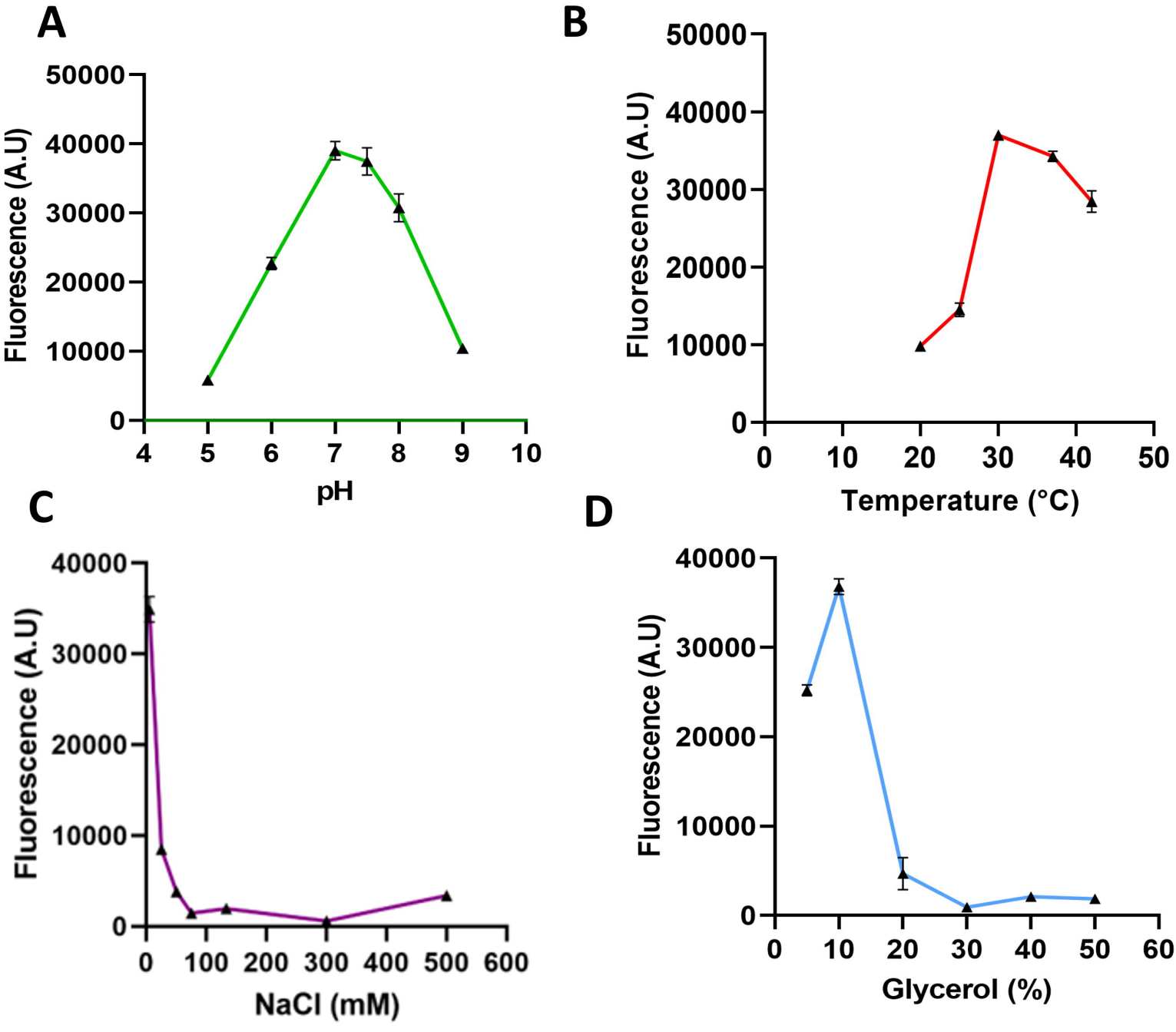
A
Fluorescence (A.U)
50000
40000
30000
20000
10000
0
4
5
6
7
8
9
10
pH
B
Fluorescence (A.U)
50000
40000
30000
20000
10000
0
0
10
20
30
40
50
Temperature (°C)
C
Fluorescence (A.U)
40000
30000
20000
10000
0
0
100
200
300
400
500
600
NaCl (mM)
D
Fluorescence (A.U)
40000
30000
20000
10000
0
0
10
20
30
40
50
60
Glycerol (%)

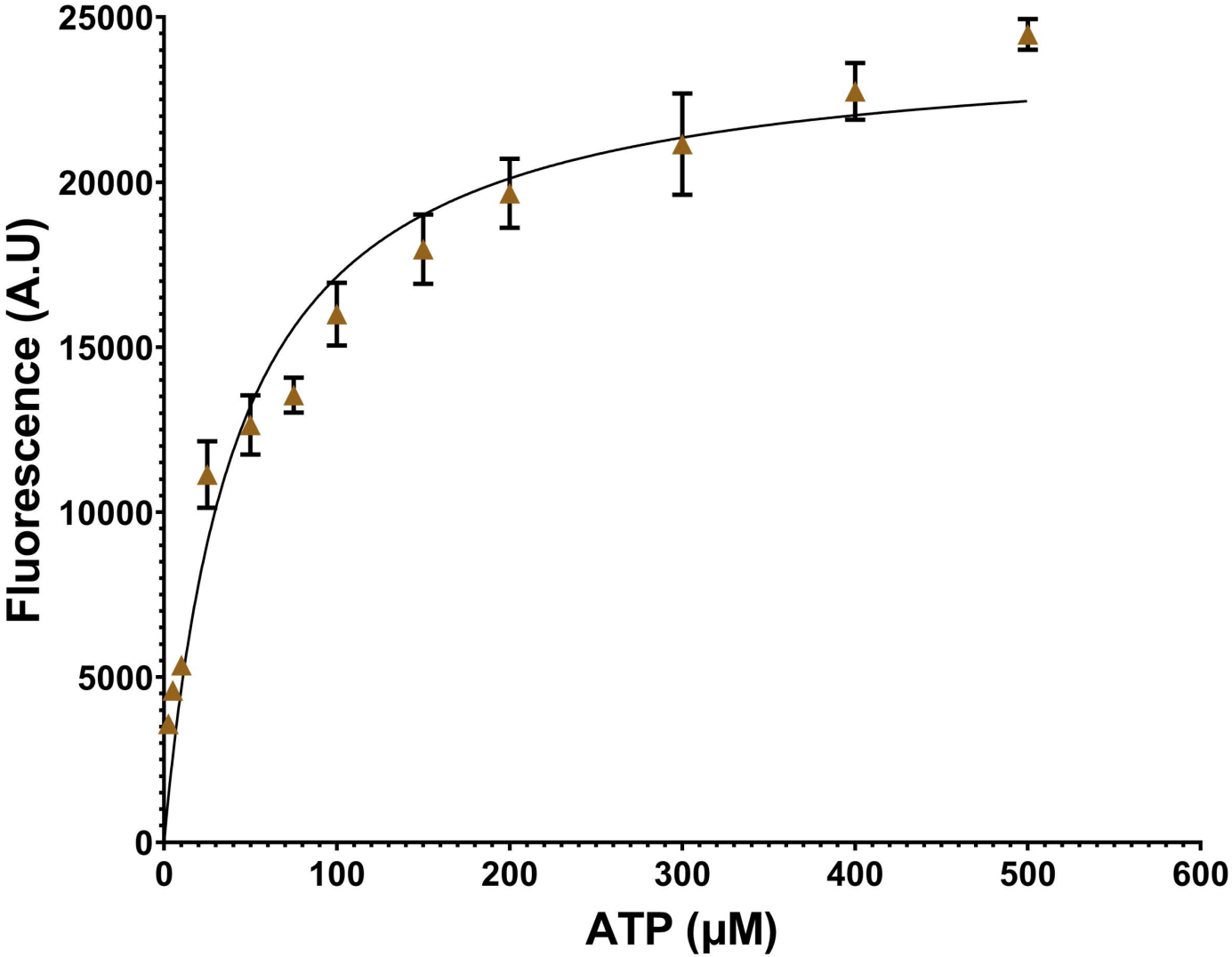
25000
20000
15000
10000
5000
0
Fluorescence (A.U)
0
100
200
300
400
500
600
ATP (μM)

Motif F

KFDV	452	VYNMMGKREKKLG----------EFGVAKGSRAIWYM	478
ALKV	452	VYNMMGKREKKLG----------EFGVAKGSRAIWYM	478
TBEV	452	VYNMMGKREKKLG----------EFGVAKGSRAIWYM	478
YEFV	452	EYNMMGKREKKLS----------EFGKAKGSRAIWYM	478
ZKV	452	VYNMMGKREKKQG----------EFGKAKGSRAIWYM	478
JAEV	453	IYNMMGKREKKPG----------EFGKAKGSRAIWFM	479
WNV	453	IYNMMGKREKKPG----------EFGKAKGSRAIWFM	479
DEN_V2	450	VYNMMGKREKKLG----------EFGKAKGSRAIWYM	476
HCV	135	DTTIMAKSEVFCVQPEKGGEKDPAKGVEKRPRVIQYP	163

	Motif G			**Motif B**		
KFDV	403	KVRSNAALGA	412	601	QRGSGQVVTYALNTL	615
ALKV	403	KVRSNAALGA	412	601	QRGSGQVVTYALNTL	615
TBEV	403	KVKSNAALGA	412	601	QRGSGQVVTYALNTL	615
YEFV	403	KVRSHAAVGA	412	601	QRGSGQVVTYALNTI	615
ZKV	403	KVRSNAALGA	412	601	QRGSGQVVTYALNTF	615
JAEV	404	KVNSNAALGA	413	602	QRGSGQVVTYALNTF	616
WNV	404	KVNSNAALGA	413	602	QRGSGQVVTYALNTF	616
DEN_V2	401	KVRSNAALGA	411	599	QRGSGQVGTYGLNTF	613
HCV	90	LTPPHSAKSK	99	279	CRASGVLTTSCGNTL	293

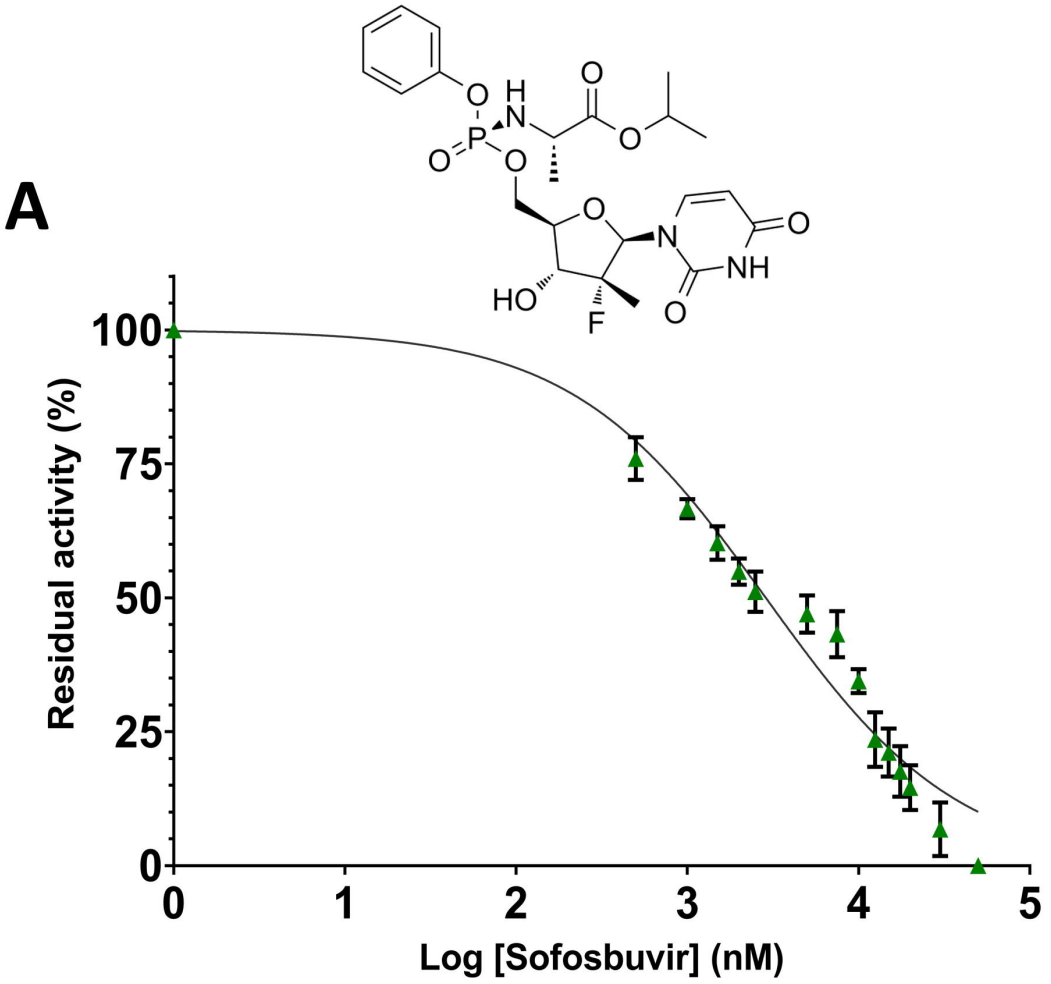
A
Residual activity (%)
100
75
50
25
0
0
1
2
3
4
5
Log [Sofosbuvir] (nM)

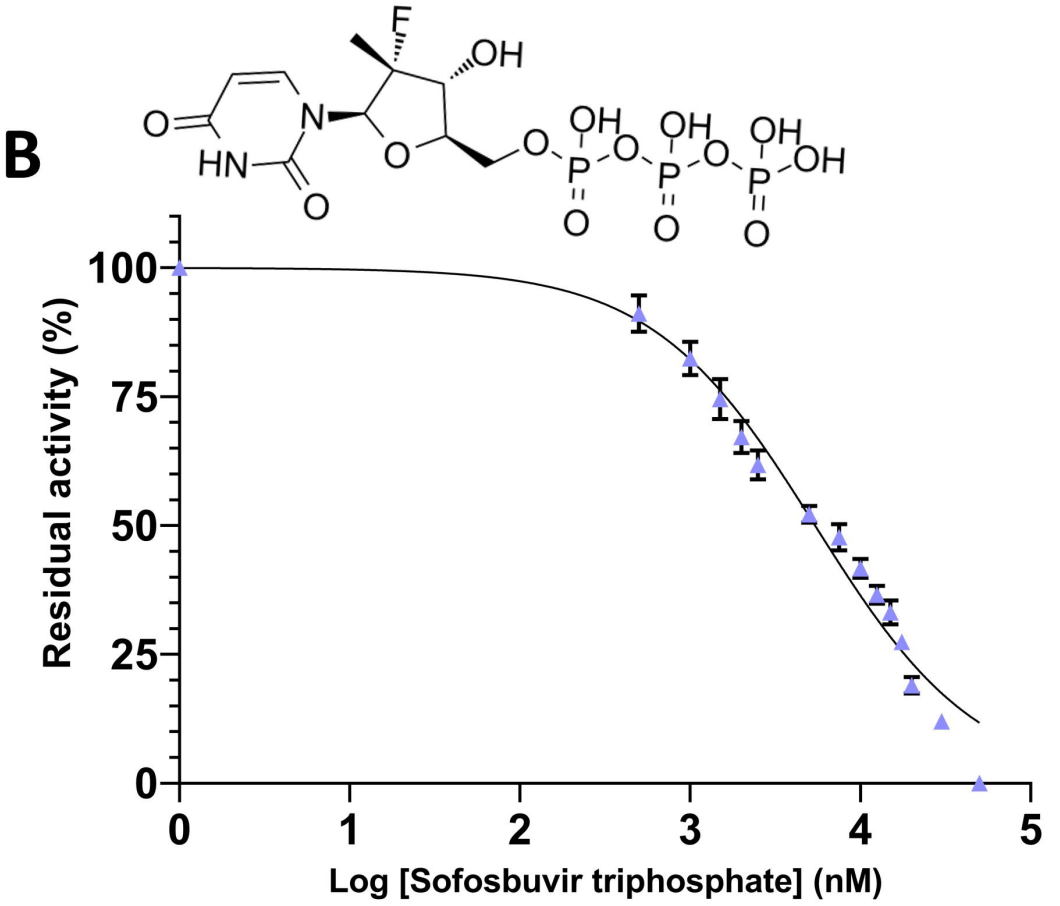
B
Residual activity (%)
100
75
50
25
0
0
1
2
3
4
5
Log [Sofosbuvir triphosphate] (nM)